Postprint of: de los Ángeles Fernandez M., de los Ángeles Sanromán M., Marks S., Makinia J., del Campo A. G., Rodrigo M., Fernandez F. J., A grey box model of glucose fermentation and syntrophic oxidation in microbial fuel cells, Bioresource Technology, Vol. 200 (2016), pp. 396-404, DOI: 10.1016/j.biortech.2015.10.010

A grey box model of glucose fermentation and syntrophic oxidation in Microbial Fuel Cells

Maria de los Ángeles Fernandez[1,2], Maria de los Ángeles Sanromán[2], Stanislaw Marks[1,3], Jacek Makinia[3], Araceli Gonzalez del Campo[1], Manuel Rodrigo[1], Francisco Jesus Fernandez[*1]

[1]University of Castilla-La Mancha, ITQUIMA, Chemical Engineering Department, Avenida Camilo José Cela S/N. 13071 Ciudad Real, Spain.

[2]University of Vigo, Department of Chemical Engineering, Isaac Newton, Vigo, Spain Building, Campus As Lagoas, Marcosende 36310 Vigo, Spain

[3]Gdansk University of Technology, Faculty of Civil and Environmental Engineering, Gabriela Narutowicza 11/12, 80-233 Gdansk, Poland.

* Corresponding author: Francisco Jesús Fernández Morales
University of Castilla-La Mancha, ITQUIMA, Chemical Engineering Dept., Avda. Camilo José Cela S/N 13071, Ciudad Real, Spain.
Tel: 0034 926 295300 (ext. 6350), Fax: 0034 926 295242.
E-mail: FcoJesus.FMorales@uclm.es

Abstract

In this work, the fermentative and oxidative processes taking place in a microbial fuel cell (MFC) fed with glucose were studied and modeled. The model accounting for the bioelectrochemical processes was based on ordinary, Monod-type differential equations. The model parameters were estimated using experimental results obtained from three H-type MFCs operated at open or closed circuits and fed with glucose or ethanol. The experimental results demonstrate that similar fermentation processes were carried out under open and closed circuit operation, with the most important fermentation products being ethanol (with a yield of 1.81 mol mol^{-1} glucose) and lactic acid (with a yield of 1.36 mol mol^{-1} glucose). A peak in the electricity generation was obtained when glucose and fermentation products coexisted in the liquid bulk. However, almost 90% of the electricity produced came from the oxidation of ethanol.

Keywords: Microbial fuel cell; glucose; fermentation; ethanol; modeling.

1. Introduction

Due to increasing energy demands and environmental concerns, the interest in the development of renewable energy sources as alternatives to fossil fuels has increased in recent years (MacKie et al., 2013). At the same time, more stringent environmental requirements for wastewater treatment are pressing for the development of more efficient treatment techniques. This phenomenon is not only an environmental concern but also an economical issue because water and wastewater systems are significant energy consumers. For example, an estimated 3-4% of U.S. electricity is consumed by the water and wastewater industry (Chandrappa & Das, 2014). In such a scenario, a reduction in treatment costs is necessary. Currently, the most important operational cost in a conventional wastewater treatment plant (WWTP) is aeration (Fernández et al., 2011a). Thus, the development of a process allowing for the oxidation of the pollutants with lower aeration requirements is of crucial importance. Currently, the most adequate technology for solving the combined energetic and environmental problem seems to be bioelectrochemical technology. Because of that, bioelectrochemical systems, including Microbial Fuel Cells (MFCs) and Microbial Electrolysis Cells (MECs), have been investigated as alternative energy sources and wastewater treatment systems (Brillas & Martínez-Huitle, 2015).

MFCs are electrochemical devices that can directly convert organic and inorganic substrates into electricity by means of a microbial culture. MFCs mimic a biological system, with the only difference being that they do not transfer electrons directly to the electron acceptor. Instead, the MFC anodofilic bacteria transfer the electron to a solid electrode as part of their respiration pathway. Then, the electron is externally conducted over the anode to the cathode, which results in the production of electricity

64 (Rao et al., 1976). Because of this ability, the interest in MFC is increasing due to its
65 dual benefit: the production of green electricity and the oxidation of wastewater
66 components without an oxygen supply (Picioreanu et al., 2008). The main advantages
67 of these devices are the mild operational conditions (neutral pH and ambient
68 temperature) and the unlimited range of potential fuels that could be used (Schröder,
69 2007), including wastes and fuels for which catalysts are currently unavailable.
70 In the MFC, one of the most widely used fuels is glucose. Glucose has been proposed
71 as an interesting renewable energy source because it is safe (non-flammable and non-
72 toxic) and its energy density (16 Mj Kg^{-1}) is lower than that of methanol or gasoline but
73 is still quite high. Moreover, glucose is a basic unit of organic compounds that
74 abundantly exist in wastewater. Therefore, glucose seems to be a powerful and
75 environmentally friendly option.
76 Glucose-rich wastewaters can be found in different industries, but the industry
77 producing the highest amounts is the agro-food industry (De Lucas et al., 2005). Agro-
78 food wastewaters are characterized by very high organic loads and biodegradability
79 (Rodríguez et al., 2007). The development of a technology capable of efficiently using
80 the glucose contained in agro-food wastewater is of crucial importance to developing
81 real applications of the MFC technologies.
82 The main drawback of the use of glucose as a fuel in the MFC is that glucose-rich
83 streams give rise to only a small current when they are used as fuel in the MFC (Kim et
84 al., 2007; Lee et al., 2008). This small current occurs because glucose is a complex
85 substrate, and glucose can be used as a substrate in a large number of non-
86 electrogenic anaerobic processes (Freguia et al., 2008).

During the operation of MFCs, multiple/parallel bioelectrochemical reactions take place. One of these simultaneous processes is fermentation. Fermentation and electrogenesis are two primary steps in bioelectrochemical systems (Premier et al., 2013). The objective of fermentation is to transform organic materials into the end products of liquids and gases through a variety of bioconversion stages (Fernández et al., 2011b). Several MFC studies have shown that fermentation and anode respiration processes are often combined (Freguia et al., 2008). Fermentative bacteria are able to ferment complex organic substrates to short-chain fatty acids (SCFA), alcohols and other fermentation products. All of these products can subsequently be oxidized to produce electricity (Kim et al., 2007). Integrating both processes in the anodic chamber may have a positive influence on the overall efficiency of wastewater treatment and the generation of electricity. Therefore, the description of the fermentation process at the anodic chamber of MFCs is of great interest.

One of the most economical and appropriate approaches to investigating the microbial behavior of and to comprehending the bioelectrochemical interactions in both MFCs and MECs is through mathematical modeling (Karimi Alavijeh et al., 2015). Modeling efforts have also been directed towards several aspects related to MFCs, evolving in recent years from simple to complex models, such as multi-species, multi-dimensional or multiscale models (Ortiz-Martínez et al., 2015). In the literature, there are papers discussing generalized models describing wastewater treatment and the associated energy production on MFC (Karimi Alavijeh et al., 2015), models of MFC biofilms and suspended cultures (Picioreanu et al., 2010a), models of inorganic pollutants and pH effects on MFC (Picioreanu et al., 2010b) and papers reviewing and classifying the existing models (Ortiz-Martínez et al., 2015).

In this context, the objective of this study was to evaluate the performance of a MFC fed with glucose in order to study the influence of the fermentation process and the syntrophic oxidation of the fermentation products generated on the performance of the MFC.

2. Materials and methods

2.1 MFC Model definition

To clarify the glucose transformations in the MFC, the fermentation process and the subsequent oxidation of the fermentation products were modelled. The model definition was based on experimental observations when studying the fermentative and subsequent oxidative processes in the H-type MFCs used in this work. These equations are presented in the form of the Petersen matrix in Table 1, and the parameters of the model are presented in Table 2. All of the kinetics expressions are based on the classical, commonly-used Monod terms (Monod, 1949). The equations address the soluble compounds involved anaerobic and electrogenic transformations. Thus, the effect of the concentration of the mediator in oxidized form was included in the electrogenic processes (Picioreanu et al., 2010a).

[TABLE 1 NEAR HERE]

[TABLE 2 NEAR HERE]

In the developed model, the reactions proposed included glucose fermentation to fermentation products (via non-electrogenic fermentation processes) and the oxidation of glucose and the fermentation products to produce electricity. The fermentation was considered to be non-electrogenic because the main fermentation products accumulated in the liquid bulk of both MFCs (open and closed circuit) correspond to those not generated by means of the electricity generation processes. On the other hand, based on the experimental results, the main electrogenic reactions were the electrogenic oxidation of glucose and the main fermentation product (i.e., ethanol) to CO_2.

When the anodic and cathodic chambers were connected via the external electrical circuit (i.e., closed circuit), the environmental conditions required for electrogenic metabolism by the organisms were obtained. In contrast, the fermentative processes, rather than the electrogenic ones, may be the predominant processes when working under open circuit conditions. Through the comparison of MFCs of both circuit types (closed and open), the fermentation and electrogenic metabolisms were discriminated.

Taking into account the similarities observed when working with the open and closed circuit MFCs, the fermentation equations proposed for the open circuit MFC were also used for the closed circuit MFC. The only difference was the existence of a lag phase when fermenting glucose to lactic acid under closed circuit conditions but not under open circuit conditions. To describe both behaviors, a switching function in the lactic acid production rate was included (see process B2 in Table 2). The different behavior of the closed circuit MFC could be explained because of the ability of the microorganisms to switch between glucose oxidation with electricity production and lactic acid generation from glucose fermentation. The switching function was based on an inhibition function proposed in the literature (Edwards, 1970). In this function, an additional term called I_x was included. This term is a Boolean function with a value of 0 for open circuit and 1 for closed circuit. The inclusion of this term allowed us to describe the differences in the fermentation under open or closed circuit conditions. Additionally, the glucose and fermentation products generated could be oxidized to carbon dioxide, thereby generating electricity. The equations describing these processes in the model are processes E1 and E2 (Table 2). A reaction-scheme of the proposed model is depicted in Figure 1.

FIGURE 1 NEAR HERE

Neither hydrogen production by fermenters nor methane production by methanogens were included in the developed model because neither methane nor hydrogen were detected in the gas phase of the H-type MFC. The lack of methane in the gas phase could be explained because of the acidification of the anodic chamber, which inhibits the activity of the methanogenic microorganisms (Fernández-Morales et al., 2010). Regarding hydrogen, its absence could be related to the seed used for the inoculation of the MFC. Acetic and formic acids only appeared in trace concentrations, in both open and closed circuit experiments, and therefore they were not included in the model.

Taking into account the processes identified, the calibration was performed in three stages. In the first stage, the calibration was focused on the non-electrogenic fermentation processes. In the second stage the electrogenic ethanol oxidation was modeled. Finally, a third stage was used to simultaneously study the whole system, including the glucose fermentation and the electrogenic glucose and ethanol consumption, as well as the associated electricity generation.

To determine the best fit of the model, mathematical calculations were performed using the Solver Tool in MS Excel. These calculations required the calculation of the minimum residual sum of squared errors, which is associated with the difference between the experimental data and the theoretical predictions of the model (de Lucas et al., 2007).

2.2 MFC Design and configuration

Dual-compartment H-type MFCs were used. The MFCs held 0.7 L in each compartment,

and the compartments were separated by a tubular central compartment into which the separator was located (see Figure 2). The separator used in this work was a 5 cm thick microporous separator, including 16 cm^3 of compacted kaolin powder (with particle diameters less than 35 microns). This separator was supported by a glass fiber filter to avoid disintegration due to the action of bulk liquid at both anodic and cathodic sides of the separator. The separator was designed to avoid the transport of microorganisms from the anodic to the cathodic chamber and to avoid the transport of oxygen from the cathodic to the anodic chamber. It must be stated that the MFC used in this work was mainly limited due to the internal resistance of the separator; therefore, the results are not directly applicable to a single-chamber MFC. The electrodes used in both the anode and the cathode were porous graphite rods (1 cm OD x 10 cm L) without any surface treatment or catalytic addition. Before the experiments, the electrodes were first soaked in deionized water for a period of 24 h. The submersible external surface of each electrode was 25.9 cm^2. The electrodes were placed at a distance of 20 cm on either side of the MFC. Cooper wires and a 120 ohm resistor were used as a contact from the electrodes. The cathode was continuously aerated by using an aquarium air pump. During the experiments, the air pump supplied 6 L min^{-1} of air at 1.5 atmospheres of pressure to the cathodic chamber.

Three identical H-type MFCs were used to study different processes, including electricity production from glucose, electricity production from the main fermentation product (ethanol), and the glucose fermentation process. In the latter case, the fermentation process was isolated from the electricity production process by disconnecting the external electrical circuit.

[FIGURE 2 NEAR HERE]

212

213 *2.3 MFC operation*

214 The anodic chamber of the MFCs were fed with a medium solution containing the
215 organic substrate, 9 g L of glucose or 3.3 g L of ethanol (depending on the test) and the
216 following trace minerals (in g L^{-1}): NH_4Cl 3.0150; KH_2PO_4 1.7550; NaCl 0.6570; Na_2SO_4
217 0.1290; $MgCl_2$ $6H_2O$ 0.2700; EDTA 0.1125; $ZnSO_4$ $7H_2O$ 0.0072; $FeSO_4$ $7H_2O$ 0.0070;
218 $MnCl_2$ $4H_2O$ 0.0056; CuCl $2H_2O$ 0.0050; $CoCl_2$ $6H_2O$ 0.0022; $CaCl_2$ 0.0014; $NiCl_2$ $6H_2O$
219 0.0011; Na_2MoO_4 $2H_2O$ $0.225 \cdot 10^{-3}$; and H_3BO_4 $0.225 \cdot 10^{-3}$. The carbon and mineral
220 solution was sterilized in an autoclave at 110 °C for 20 min. A high organic substrate
221 concentration was used to identify non-electrogenic anaerobic reactions and also to
222 maintain a longer energy production in the batch microbial fuel cell. The cathodic
223 chamber was fed with demineralized water.

224 The anodic chambers of the MFCs were seeded two days after the start-up of the
225 MFCs with a selectively enriched mixed culture taken from the effluent of a working
226 MFC (Gonzalez del Campo et al., 2013). By working in this way, the absence of
227 electricity generation before the seed of the MFC was verified, serving these data as
228 abiotic control data.

229 All of the experiments were conducted in batch mode. The experiments were
230 continued until there was no significant change in the measured quantities. The
231 contents in the anode and cathode chambers were continuously homogenized by
232 means of magnetic stir bars rotating at 80 rpm. The power output was monitored by
233 measuring voltage with an external resistor (120 ohms) connected between the
234 electrodes.

235

236 *2.4 Analytical methods and calculations*

237 Aqueous samples were collected from each MFC and then immediately centrifuged
238 (12000 rpm) and filtered through a 0.45 µm membrane filter. Once filtered, the
239 samples were analyzed or preserved frozen, according to the procedures described in
240 the literature (Eaton et al., 2005).

241 Glucose concentrations were measured by HPLC (Agilent) with a refractive index
242 detector (series 1200). A Zorbax Carbohydrate Column (4.6 x 150 mm, 5-micron) was
243 used to separate the components at 35 °C using a mobile phase composed of 75%
244 acetonitrile and 25% water v/v and a flow rate of 1.5 cm^3 min^{-1}. Furthermore, lactic
245 acid was determined from centrifuged and filtered samples by HPLC (Agilent) equipped
246 with UV-DAD and Zorbax SB-Aq (4.6 x 150 mm, 5-micron). The mobile phase was a
247 buffer at pH 2 (0.05 M phosphate). SCFA (acetic, propionic and butyric) and ethanol
248 contents were determined from a centrifuged (12000 rpm) and filtered sample (0.45
249 µm membrane) by gas chromatography (Perkin Elmer) with a flame ionization detector
250 (FID) using a Crossbond Carbowax Column (15 m x 0.32 mm ID, 0.25 mm df). The initial
251 temperature of the oven was 140 °C, which held for for 1.5 min, and the temperature
252 was raised at 25 °C min^{-1} until 190 °C, where it was maintained for 2 min. The
253 temperature of the injector and detector were 200 °C and 230 °C, respectively.
254 Nitrogen was used as the carrier gas. More information can be found elsewhere
255 (Fernández-Morales et al., 2010; Infantes et al., 2011). pH values were determined
256 using a Crison GLP-22 pH probe (Crison Instruments S.A., Barcelona, Spain).

257 Bioelectrochemical calculations were carried out based on the procedures outlined in
258 the literature (Logan et al., 2006). Potential (V) measurements were recorded with an
259 auto range digital multimeter (Model 2700, Keithley Instrument, OH, USA). Coulombic

efficiency (CE), defined as the ratio of the total coulombs actually transferred to the anode from the substrate to the maximum possible coulombs if all substrate removal produces the electrical current (Logan et al., 2006), was calculated by integrating the current over time and taking into account the total Coulombs associated with the COD removed in the same period of time.

$$CE = \frac{M \int_0^t I \, dt}{F \, b \, V \, \Delta COD}$$

where M is the molecular weight of oxygen (32), I corresponds to the current intensity generated, F is Faraday's constant (96.485 C mol^{-1} e^-), b represents the number of electrons exchanged per mole of COD removed (4), V is the volume of liquid in the anode compartment (0.7 L), and ΔCOD depicts the change in theoretical COD concentration over the period of time. The COD concentrations were theoretically calculated based on the substrate concentration in the bulk liquid. In this way, it is possible to isolate the contribution of each product in every process. To ratify the accuracy of the theoretical COD calculations, the actual COD concentration of each sample was experimentally determined and compared with the theoretical concentration, with the error in all cases being lower than 8%. The gas composition was analyzed by a multi-component gas analyzer (Rosemount Analytical NGA 2000 MLT, Emerson).

3. Results and Discussion

Before the study and modeling of the results, the mass balance in all the experiments performed was verified. Table 3 presents the carbon balance in the glucose-fed MFC (open and closed circuit) and the ethanol-fed MFC. As seen from Table 3, the carbon recovery was approximately 90%.

[TABLE 3 NEAR HERE]

3.1 Open circuit MFC

To isolate and to study the fermentative processes taking place in the H-type MFC, an open circuit experiment was performed. Working in this way, the glucose was fermented but not oxidized by electroactive microorganisms. During the operation, the liquid bulk of the anodic chamber was analyzed, and the concentrations of the main compounds were determined. The experimental results obtained are presented in Figure 3.

[FIGURE 3 NEAR HERE]

It can be seen in Figure 3 that glucose was fully consumed after approximately 15 d. Regarding the glucose consumption, it must be noted that a reduction in pH was observed from neutrality to pH values near 5.5, which indicates the existence of the fermentation process. Several fermentation products appeared as a result of the fermentation process. The main fermentation products were ethanol and lactic acid, accounting for more than 95% of the fermentation products generated. In addition, acetic and formic acids appeared in trace concentrations (data not shown). The

maximum concentrations of ethanol and lactic acids reached approximately 6.7 and 3.4 g COD L^{-1}, respectively.

With the aim of using this information for the description of the processes taking place in the closed circuit H-type MFC, the model equations corresponding to the glucose fermentation processes were fitted to the experimental data. From the fitting, the main kinetics and stoichiometric parameters were determined. The yields of the main fermentation products, ethanol and lactic acid, were 0.88 and 0.68 g COD per g COD of glucose consumed, respectively, and the maximum specific uptake rates were 2.3 g COD (g COD d)$^{-1}$ and 1.2 g COD (g COD d)$^{-1}$ for ethanol and lactic acid, respectively. The glucose half-saturation coefficient (K_s) was 1.93 g COD L^{-1} in both cases. As seen in Figure 3, the model accurately predicts the substrate and product concentrations along the fermentation experiment.

The equations proposed and the parameter values obtained were subsequently used to fit the closed circuit experimental data set obtained when glucose was used for the electricity generation.

3.2 Closed circuit MFC

With the aim to studying the fermentative and electrogenic processes simultaneously occurring in the H-type MFC, a closed circuit experiment with glucose and feedstock was performed. During the experiment, the patterns of change of the main variables were determined.

3.2.1 Power generation and theoretical COD removal

Before the inoculation, the anodic chamber of the H-type MFC was operated with the sterilized wastewater in the absence of biocatalyst for a period of 2 d. During this

period, the electricity generation was negligible. Subsequently, the H-type MFC was seeded. The H-type MFC was continuously operated in a batch mode for three months. The experimental data presented in Figure 4 illustrate the voltage generation of the H-type MFC and the theoretical COD removal rate in the liquid bulk.

[FIGURE 4 NEAR HERE]

As seen in Figure 4, the electricity generation was proportional to the theoretical COD removal rate in the system. In this figure, several sections can be identified. Initially, the system presented an exponential increase of the voltage, which could be explained because of the high consumption rate of the substrates by the microorganisms in the anodic chamber. A maximum voltage output of 12.0 mV was observed after 15 d of the start-up, which corresponds to a CE of approximately 1.5%.

After achieving the maximum in the voltage exerted, the voltage gradually dropped to approximately 6.0 mV. Over more than 40 d, the voltage was maintained at approximately 6.0 mV, with an average CE of approximately 2.5%. This result could be explained because of the almost constant COD consumption rate of approximately 0.3 g COD (g COD d)$^{-1}$. The low CE can be explained by a very high glucose concentration (9.6 g COD L^{-1}) in the anodic chamber. This finding could be related to the fact that the conventional anaerobic organisms outcompete the electrogenic ones when working at very high glucose concentrations. In the literature (Velasquez-Orta et al., 2011), similar results were reported for studies working with high glucose concentrations. Finally, after approximately 70 d of operation, the voltage decreased again to approximately 0.5 mV, which may be related to endogenous electricity generation.

3.2.2 Substrate transformation

Regarding the use of glucose as a fuel, it is remarked that the slight pH reduction observed (from 7 to approximately 6) and the long-lasting voltage generation over more than 100 d (even when the glucose was exhausted after only 20 d) indicated that the glucose added to the MFC was transformed in the anodic chamber. Because of the importance of the fermentation process in the MFC (Lee et al., 2008), the glucose concentration and the fermentation product concentrations were monitored (see Figure 5). In Figure 5, it can be seen that the MFC performed fermentation apart from power generation.

[FIGURE 5 NEAR HERE]

During the first 20 d of the operation of the closed circuit MFC, the main transformations can be explained because of the glucose fermentation to ethanol and lactic acid, as occurred in the open circuit MFC.

As seen in Figure 5, the glucose was consumed in approximately 20 d. During this period, several fermentation products appeared in the anodic liquid bulk, with ethanol and lactic acid being the most relevant, but acetic and formic acids also appeared, similar to the open circuit MFC. Considering the comparison of the production of the fermentation products in the open and closed circuit MFCs, the existence of a lag phase in the lactic acid production under closed circuit conditions is remarkable. To account for this difference, a switch function in the lactic acid production rate (see process B2 in Table 2) was included. Furthermore, a slightly higher formic acid production must be noted when working under closed circuit conditions. In the closed circuit, formic acid was generated at a rate of approximately 0.03 g COD (g COD d)$^{-1}$ and with a yield of 0.08 mol COD of formic acid per mol COD of glucose. This higher production could be explained because of the higher pH in the bulk liquid when

operating under closed circuit conditions. In the literature (Temudo et al., 2007), it has been reported that formic acid production is favored at high pH values. The higher pH values observed under closed circuit conditions could be explained by the acid oxidation by electrogenic organisms and proton consumption in the cathodic compartment of the MFC.

In principle, because the fermentation process takes place in the anodic chamber, some of the electricity generation during the first 20 d of the experiment could be explained because of the electrogenic fermentation of glucose (Catal et al., 2011). This event could be possible in an MFC because there are different fermentation pathways that could be divided into two groups, including the electricity generation processes (Reactions (1-3)) and the conventional fermentation processes (Fang & Liu, 2002; Fang et al., 2002). The latter processes do not generate electricity (Reactions (4-8).

Electrogenic fermentative processes (EFP)

$$C_6H_{12}O_6 + 2H_2O \rightarrow 2CH_3COOH + 2CO_2 + 8H^+ + 8e^- \quad (1)$$

$$C_6H_{12}O_6 \rightarrow (CH_3)_2CHCOOH + 2CO_2 + 4H^+ + 4e^- \quad (2)$$

$$C_6H_{12}O_6 \rightarrow CH_3CH_2COOH + CH_3COOH + CO_2 + 2H^+ + 2e^- \quad (3)$$

Non-electrogenic fermentative processes (NEFP)

$$C_6H_{12}O_6 + 2H_2O \rightarrow 2CH_3COOH + 2CO_2 + 4H_2 \quad (4)$$

$$C_6H_{12}O_6 \rightarrow (CH_3)_2CHCOOH + 2CO_2 + 2H_2 \quad (5)$$

$$C_6H_{12}O_6 \rightarrow CH_3CH_2COOH + CH_3COOH + CO_2 + H_2 \quad (6)$$

$$C_6H_{12}O_6 \rightarrow 2C_2H_5OH + 2CO_2 \quad (7)$$

$$C_6H_{12}O_6 \rightarrow 2\ CH_3CHOHCOOH \quad (8)$$

Additionally, the electricity generation in the MFC could also be due to the direct conversion of glucose to CO_2 (Reaction (9)) and the conversion of the fermentation products generated to CO_2 (Reactions (10-14). The sum of all of these contributions could explain why the peak in the electricity generation was reached at 15 d after the start-up of the MFC. After that peak, the glucose was exhausted; therefore, only the fermentation products could have been used for electricity generation.

Electrogenic oxidative processes (EOP)

$$C_6H_{12}O_6 + 12H_2O \rightarrow 6CO_2 + 24H^+ + 24e^- \quad (9)$$

$$CH_3COOH + 2H_2O \rightarrow 2CO_2 + 8H^+ + 8e^- \quad (10)$$

$$(CH_3)_2CHCOOH + 6H_2O \rightarrow 4CO_2 + 20H^+ + 20e^- \quad (11)$$

$$CH_3CH_2COOH + 4H_2O \rightarrow 3CO_2 + 14H^+ + 14e^- \quad (12)$$

$$C_2H_5OH + 3H_2O \rightarrow 2CO_2 + 12H^+ + 12e^- \quad (13)$$

$$CH_3CHOHCOOH + 3H_2O \rightarrow 3CO_2 + 12H^+ + 12e^- \quad (14)$$

Taking the above reactions into account, the voltage produced during the first stage (see Figure 4) could be related to the electrogenic fermentation of glucose, the non-electrogenic glucose fermentation and the subsequent electrogenic oxidation of the fermentation products, or it could be due to the electrogenic oxidation of glucose to CO_2.

In this work, it is important to note that the main fermentation products accumulated in the liquid bulk of both MFCs (open and closed circuit), corresponding to those not generated by means of the electricity generation processes (reactions 7-8). There are

421 two possible explanations for this finding, including a negligible contribution of these
422 electricity generating processes in the closed circuit MFC or a quick consumption of the
423 fermentation products generated by means of the electrogenic fermentative
424 processes. In this work, the latter explanation was refused based on the conclusions
425 reported in the literature when fermenting monosaccharides in MFCs (Catal et al.,
426 2011).
427 During the second stage (see Figure 4), the main reaction generating electricity was
428 the oxidation of the fermentation products previously generated, particularly ethanol,
429 which was the main fermentation product consumed. In this work, lactic acid was not
430 consumed, which is in accordance with Thurston (1985), who reported the generation
431 of lactic acid in a MFC without further utilization to generate electricity under
432 anaerobic conditions (Thurston et al., 1985).
433 Finally, the third stage (see Figure 4), which is characterized by a very low voltage
434 generation, could be explained due to the oxidation of traces of SCFA presented in the
435 liquid bulk or to endogenous electricity generation. However, taking the almost
436 negligible soluble COD removal rate into account, the most probable explanation is
437 endogenous electricity generation.
438 Because of the simultaneous generation and consumption of ethanol in the closed
439 circuit MFC, it was considered interesting to uncouple the generation/consumption of
440 ethanol and determine the kinetics and stoichiometric parameters for ethanol
441 consumption in a specific experiment. Hence, an additional experiment was performed
442 in an identical H-type MFC fed with ethanol at 6.0 g COD L^{-1}. In this experiment, the
443 ethanol consumption and the electricity generation were studied, and the results are
444 presented in Figure 6.

445 [FIGURE 6 NEAR HERE]

446 It can be seen in Figure 6 that the system started to degrade the ethanol and produce
447 electricity after a short acclimatization period. The ethanol degradation rate was
448 almost constant over the course of the experiment. Once the electricity generation
449 started, the voltage generated increased, reaching a maximum voltage generation of
450 approximately 7 mV. This voltage generation was maintained for approximately 70 d
451 and then decreased, reaching a new steady state at approximately 1 mV. In the
452 absence of substrate, this result can only be explained by endogenous electrogenic
453 generation.

454 With the aim of determining the main kinetics and stoichiometric parameters of the
455 electrogenic ethanol oxidation, the equations describing the ethanol consumption and
456 the coupled electricity generation (see process E2 in Table 1) were fitted to the
457 experimental results, with the ethanol degradation rate being 0.3 g COD (g COD d)$^{-1}$
458 and the half-saturation coefficient being 0.96 g COD L^{-1}. The K_S value obtained is very
459 similar to that referenced in the literature (Kim et al., 2007). The equations proposed,
460 as well as the parameter values obtained, were subsequently used for fitting the
461 closed circuit experimental data obtained when glucose was used for the electricity
462 generation.

463 Once the kinetics and stoichiometric parameters of the fermentation, as well as those
464 of the ethanol oxidation and the associated electricity production, were determined,
465 all of the equations of the MFC model were used to simulate the experimental data set
466 obtained in the experiment performed with glucose in the closed circuit H-type MFC.
467 The kinetics and stoichiometric parameters obtained through the fermentation and in
468 the ethanol electrogenic oxidation tests were used in the model. The obtained results

accurately predict the evolution of the substrate, the fermentation product profiles and the electricity production in the H-type MFC, as seen from the model predictions and the actual data presented in Figures 5 and 6. The values of the main kinetics and stoichiometric parameters obtained from the fitting are summarized in Table 4. It was only necessary to include a small amount of glucose oxidation to accurately fit the electricity production.

From the obtained results, it is interesting to note the almost negligible oxidation rate of glucose by anodophilic organisms: 0.03 g COD (g COD d)$^{-1}$. A possible explanation is that the direct anodic oxidation of glucose by pure electrogenic cultures, which has been previously observed (Chaudhuri & Lovley, 2003), may not be the most important pathway when working with mixed cultures (Freguia et al., 2008). This phenomenon could be due to the very low concentration of electrogenic microorganisms in the mixed culture. Another possible explanation is the lower affinity and lower maximum consumption rate of the substrate by the electrogenic microorganisms compared with the conventional ones. This notion was confirmed when comparing the carbon consumption rate in the fermentation process with the electrogenic ethanol and glucose oxidation. The carbon consumption rate during the glucose fermentation process was approximately 16 mmol C (L d)$^{-1}$, whereas the carbon consumption rate during the electrogenic ethanol and glucose consumption was ten times lower (approximately 1.5 mmol C (L d)$^{-1}$).

The biomass growth in the system was fitted using an endogenous decay rate of 0.02 d^{-1} and a biomass yield of 0.07 g COD (g COD)$^{-1}$ (Romli et al., 1995). According to theoretical values, the oxidative aerobic biomass growth accounted for approximately 40% of the carbon consumption, and the anaerobic one accounted for approximately

493 5%. The value proposed in this work corresponds to a weighted value between both
494 processes, i.e., the anaerobic one (fermentative) and the oxidative one (electrogenic).
495 Similar values for the biomass growth in MFCs have been observed in previous studies
496 (Kim et al., 2011).
497 In the closed systems fed with glucose or ethanol, the electrons transported through
498 the circuit represented a small portion, ranging from 1 to 3%. This finding could be
499 explained by the loss of MFC electrons by overpotential, ohmic resistance and the
500 inefficient oxidation of fermentation products and glucose.
501 [TABLE 4 NEAR HERE]
502
503 *3.3 Model validation*
504 Once the calibration procedure was finished, the developed model was compared and
505 validated using data from a new experiment. During the validation, a satisfactory
506 agreement was obtained between the measured and predicted values. The goodness
507 of fit was determined by the Mean Relative Squared Error (MRSE) criterion. The MRSE
508 values obtained during the calibration and validation stages are presented in Table 5.
509 The obtained results show that the model accuracy was maintained during the
510 validation stage, with a MRSE value of 12.3%, a value very similar to that obtained
511 during the calibration of the model.
512 [TABLE 5 NEAR HERE]

CONCLUSIONS

In this work, a model describing the evolution of a MFC fed with high glucose concentrations was developed. Comparing open and closed circuit operation of the MFC, similar reaction extensions and product distributions of the fermentation process were observed. From the obtained results, the importance of the fermentation process in electricity production was shown by the high ethanol consumption rate by electrogenic organisms (0.3 g COD (g COD d)$^{-1}$) compared with that of the glucose (0.03 g COD (g COD d)$^{-1}$). In terms of electricity generation, ethanol contributed to approximately 90% the production, whereas glucose accounted for only 10% of the production.

Acknowledgements

This research was funded by the Ministerio de Economía y Competitividad of the Spanish government through the project CTQ2013-49748-EXP.

References

Brillas, E., Martínez-Huitle, C.A. 2015. Decontamination of wastewaters containing synthetic organic dyes by electrochemical methods. An updated review. *Applied Catalysis B: Environmental*, **166-167**, 603-643.

Catal, T., Fan, Y., Li, K., Bermek, H., Liu, H. 2011. Utilization of mixed monosaccharides for power generation in microbial fuel cells. *Journal of Chemical Technology and Biotechnology*, **86**(4), 570-574.

Chandrappa, R., Das, D.B. 2014. *Sustainable Water Engineering : Theory and Practice*. Wiley, Chichester.

Chaudhuri, S.K., Lovley, D.R. 2003. Electricity generation by direct oxidation of glucose in mediatorless microbial fuel cells. *Nature Biotechnology*, **21**(10), 1229-1232.

De Lucas, A., Rodriguez, L., Villasenor, J., Fernandez, F.J. 2005. Denitrification potential of industrial wastewaters. *Water Research*, **39**(15), 3715-3726.

de Lucas, A., Rodríguez, L., Villaseñor, J., Fernández, F.J. 2007. Fermentation of agro-food wastewaters by activated sludge. *Water Research*, **41**(8), 1635-1644.

Eaton, A.D., Clesceri, L.S., Rice, E.W., Greenberg, A.E., Franson, M.A.H., American Public Health Association., American Water Works Association., Water Environment Federation., APHA., AWWA., WEF. 2005. *Standard methods for the examination of water and wastewater*. *21st ed*. American Public Health Association, Washington.

Edwards, V.H. 1970. The influence of high substrate concentrations on microbial kinetics. *Biotechnology and Bioengineering*, **12**(5), 679-712.

Fang, H.H.P., Liu, H. 2002. Effect of pH on hydrogen production from glucose by a mixed culture. *Bioresource Technology*, **82**(1), 87-93.

Fang, H.H.P., Liu, H., Zhang, T. 2002. Characterization of a hydrogen-producing granular sludge. *Biotechnology and Bioengineering*, **78**(1), 44-52.

Fernández, F.J., Castro, M.C., Rodrigo, M.A., Cañizares, P. 2011a. Reduction of aeration costs by tuning a multi-set point on/off controller: A case study. *Control Engineering Practice*, **19**(10), 1231-1237.

Fernández, F.J., Villaseñor, J., Infantes, D. 2011b. Kinetic and stoichiometric modelling of acidogenic fermentation of glucose and fructose. *Biomass and Bioenergy*, **35**(9), 3877-3883.

Fernández-Morales, F.J., Villaseñor, J., Infantes, D. 2010. Modeling and monitoring of the acclimatization of conventional activated sludge to a biohydrogen producing culture by biokinetic control. *International Journal of Hydrogen Energy*, **35**(20), 10927-10933.

Freguia, S., Rabaey, K., Yuan, Z., Keller, J. 2008. Syntrophic processes drive the conversion of glucose in microbial fuel cell anodes. *Environmental Science and Technology*, **42**(21), 7937-7943.

Gonzalez del Campo, A., Lobato, J., Cañizares, P., Rodrigo, M.A., Fernandez Morales, F.J. 2013. Short-term effects of temperature and COD in a microbial fuel cell. *Applied Energy*, **101**, 213-217.

Infantes, D., González Del Campo, A., Villaseñor, J., Fernández, F.J. 2011. Influence of pH, temperature and volatile fatty acids on hydrogen production by acidogenic fermentation. *International Journal of Hydrogen Energy*, **36**(24), 15595-15601.

Karimi Alavijeh, M., Mardanpour, M.M., Yaghmaei, S. 2015. A generalized model for complex wastewater treatment with simultaneous bioenergy production using the microbial electrochemical cell. *Electrochimica Acta*, **167**, 84-96.

Kim, J.R., Jung, S.H., Regan, J.M., Logan, B.E. 2007. Electricity generation and microbial community analysis of alcohol powered microbial fuel cells. *Bioresource Technology*, **98**(13), 2568-2577.

581 Kim, K.Y., Chae, K.J., Choi, M.J., Ajayi, F.F., Jang, A., Kim, C.W., Kim, I.S. 2011. Enhanced
582 Coulombic efficiency in glucose-fed microbial fuel cells by reducing metabolite
583 electron losses using dual-anode electrodes. *Bioresource Technology*, **102**(5), 4144-
584 4149.
585 Lee, H.S., Parameswaran, P., Kato-Marcus, A., Torres, C.I., Rittmann, B.E. 2008. Evaluation of
586 energy-conversion efficiencies in microbial fuel cells (MFCs) utilizing fermentable and
587 non-fermentable substrates. *Water Research*, **42**(6-7), 1501-1510.
588 Logan, B.E., Hamelers, B., Rozendal, R., Schröder, U., Keller, J., Freguia, S., Aelterman, P.,
589 Verstraete, W., Rabaey, K. 2006. Microbial fuel cells: Methodology and technology.
590 *Environmental Science and Technology*, **40**(17), 5181-5192.
591 MacKie, D.M., Liu, S., Benyamin, M., Ganguli, R., Sumner, J.J. 2013. Direct utilization of
592 fermentation products in an alcohol fuel cell. *Journal of Power Sources*, **232**, 34-41.
593 Monod, J. 1949. THE GROWTH OF BACTERIAL CULTURES. *Annual Review of Microbiology*, **3**,
594 371-394.
595 Ortiz-Martínez, V.M., Salar-García, M.J., de los Ríos, A.P., Hernández-Fernández, F.J., Egea, J.A.,
596 Lozano, L.J. 2015. Developments in microbial fuel cell modeling. *Chemical Engineering*
597 *Journal*, **271**, 50-60.
598 Picioreanu, C., Katuri, K.P., Head, I.M., Van Loosdrecht, M.C.M., Scott, K. 2008. Mathematical
599 model for microbial fuel cells with anodic biofilms and anaerobic digestion. in: *Water*
600 *Science and Technology*, Vol. 57, pp. 965-971.
601 Picioreanu, C., Katuri, K.P., Van Loosdrecht, M.C.M., Head, I.M., Scott, K. 2010a. Modelling
602 microbial fuel cells with suspended cells and added electron transfer mediator. *Journal*
603 *of Applied Electrochemistry*, **40**(1), 151-162.
604 Picioreanu, C., van Loosdrecht, M.C.M., Curtis, T.P., Scott, K. 2010b. Model based evaluation of
605 the effect of pH and electrode geometry on microbial fuel cell performance.
606 *Bioelectrochemistry*, **78**(1), 8-24.
607 Premier, G.C., Kim, J.R., Massanet-Nicolau, J., Kyazze, G., Esteves, S.R.R., Penumathsa, B.K.V.,
608 Rodríguez, J., Maddy, J., Dinsdale, R.M., Guwy, A.J. 2013. Integration of biohydrogen,
609 biomethane and bioelectrochemical systems. *Renewable Energy*, **49**, 188-192.
610 Rao, J.R., Richter, G.J., Von Sturm, F., Weidlich, E. 1976. The performance of glucose electrodes
611 and the characteristics of different biofuel cell constructions. *Bioelectrochemistry and*
612 *Bioenergetics*, **3**(1), 139-150.
613 Rodríguez, L., Villaseñor, J., Fernández, F.J. 2007. Use of agro-food wastewaters for the
614 optimisation of the denitrification process. in: *Water Science and Technology*, Vol. 55,
615 pp. 63-70.
616 Romli, M., Keller, J., Lee, P.L., Greenfield, P.F. 1995. Model prediction and verification of a two-
617 stage high-rate anaerobic wastewater treatment system subjected to shock loads.
618 *Process Safety and Environmental Protection: Transactions of the Institution of*
619 *Chemical Engineers, Part B*, **73**(2), 151-154.
620 Schröder, U. 2007. Anodic electron transfer mechanisms in microbial fuel cells and their energy
621 efficiency. *Physical Chemistry Chemical Physics*, **9**(21), 2619-2629.
622 Temudo, M.F., Kleerebezem, R., Van Loosdrecht, M. 2007. Influence of the pH on (Open) mixed
623 culture fermentation of glucose: A chemostat study. *Biotechnology and*
624 *Bioengineering*, **98**(1), 69-79.
625 Thurston, C.F., Bennetto, H.P., Delaney, G.M. 1985. Glucose metabolism in a microbial fuel cell.
626 Stoichiometry of product formation in a thionine-mediated Proteus vulgaris fuel cell
627 and its relation to coulombic yields. *Journal of General Microbiology*, **131**(6), 1393-
628 1401.
629 Velasquez-Orta, S.B., Yu, E., Katuri, K.P., Head, I.M., Curtis, T.P., Scott, K. 2011. Evaluation of
630 hydrolysis and fermentation rates in microbial fuel cells. *Applied Microbiology and*
631 *Biotechnology*, **90**(2), 789-798.

632

Process \ Components	1 Glucose	2 Ethanol	3 Lactic	4 Acetic	5 Butyric	6 Formic	7 H_2	8 IC	9 Electricity	10 Process rate
Biological conversion										
(B1) Ethanol production	-1	$(1-Y_b)f_{e,g}$						$-\sum C_i v_{i,B1}$		$k_{G,E}\frac{S_G}{K_{S_G}+S_G}X$
(B2) Lactic production	-1		$(1-Y_b)f_{l,g}$							$k_{G,L}\frac{S_G}{K_{S_G}+S_G}X\left[exp\left(\frac{K_G-S_G}{K_{S_G}}I_X\right)\right]$
(B3) Acetic production	-1			$(1-Y_b)f_{a,g}$			$(1-Y_b)f_{H2a,g}$	$-\sum C_i v_{i,B3}$		$k_{G,Ac}\frac{S_G}{K_{S_G}+S_G}X$
(B4) Butyric production	-1				$(1-Y_b)f_{b,g}$		$(1-Y_b)f_{H2b,g}$	$-\sum C_i v_{i,B4}$		$k_{G,B}\frac{S_G}{K_{S_G}+S_G}X$
(B5) Formic production						$(1-Y_b)f_{j,IC}$	-1	$-\sum C_i v_{i,B5}$		$K_{IC,E}\frac{S_{IC}}{K_{S_{IC}}+S_{IC}}X$
Electrochemical conversion										
(E1) Electrogenic glucose oxidation	-1							$-\sum C_i v_{i,E1}$	$(1-Y_b)\gamma_{e^-,COD}$	$k_{G,e^-}\frac{S_G}{K_{S_G}+S_G}\frac{S_{Mox}}{K_{Mox}+S_{Mox}}X$
(E2) Electrogenic ethanol oxidation		-1						$-\sum C_i v_{i,E2}$	$(1-Y_b)\gamma_{e^-,COD}$	$k_{E,e^-}\frac{S_E}{K_{S_E}+S_E}\frac{S_{Mox}}{K_{Mox}+S_{Mox}}X$

Parameter	Description	Unit
Biological Conversion		
S_G	Glucose concentration	g COD · L^{-1}
S_E	Ethanol concentration	g COD · L^{-1}
S_{Mox}	Oxidised mediator concentration	g COD · L^{-1}
X	Biomass concentration	g COD · L^{-1}
Y_b	Biomass yield coefficient	g COD Biomass · (g COD glucose)$^{-1}$
$f_{product,substrate}$	Catabolic yield of product on substrate	g COD product · (g COD substrate)$^{-1}$
$k_{G,E}$	Glucose to Ethanol fermentation rate	g COD Glucose · (g COD biomass·d)$^{-1}$
$k_{G,L}$	Glucose to Lactic acid fermentation rate	g COD Glucose · (g COD biomass·d)$^{-1}$
$k_{G,Ac}$	Glucose to Acetic acid fermentation rate	g COD Glucose · (g COD biomass·d)$^{-1}$
$k_{G,B}$	Glucose to Butyric acid fermentation rate	g COD Glucose · (g COD biomass·d)$^{-1}$
K_{S_G}	Monod half-saturation coefficient for glucose	g COD Glucose · L^{-1}
K_{S_E}	Monod half-saturation coefficient for ethanol	g COD Ethanol · L^{-1}
K_{Mox}	Monod half-saturation coefficient for oxidised mediator	g COD Oxidised mediator · L^{-1}
K_G	Glucose switching constant	g COD Glucose · L^{-1}
C_i	Carbon content of component i	mole C · g COD^{-1}
v_i	Rate coefficient for component I on process j	g COD · m^{-3}
I_X	Open-closed circuit Boolean switching function	
Electrochemical Conversion		
k_{G,e^-}	Electrogenic Glucose oxidation rate	g COD Glucose · (g COD biomass·d)$^{-1}$
k_{E,e^-}	Electrogenic Ethanol oxidation rate	g COD Ethanol · (g COD biomass·d)$^{-1}$
$\gamma^{e^-}_{COD}$	Electricity generation from COD oxidation	12060 Coulombs · g COD^{-1}

	Glucose open circuit		Glucose closed circuit	
	Carbon Balance		Carbon Balance	
	C mmol	Fraction %	C mmol	Fraction %
Amount Added				
Glucose	268.09	100.00	257.25	100.00
Final recovery				
Ethanol	95.20	35.51	0.00	0.00
Lactic acid	69.30	25.85	69.51	27.02
Formic acid	1.40	0.52	4.20	1.63
Acetic acid	0.35	0.13	0.56	0.22
Butyric acid	0.00	0.00	0.03	0.01
Carbon dioxide	45.85	17.10	139.37	54.18
Biomass growth	20.20	7.53	18.34	7.13
Total recovery	***232.30***	***86.65***	***232.01***	***90.19***

Parameter	Value	Parameter	Value	Parameter	Value
Biological Conversion				***Electrochemical Conversion***	
Y_b	0.07 g COD · (g COD)$^{-1}$	$f_{H2b,g}$	0.17 g COD · (g COD)$^{-1}$	k_{m,Ee^-}	0.3 g COD · (g COD·d)$^{-1}$
$f_{e,g}$	0.88 g COD · (g COD)$^{-1}$	$k_{G,E}$	2.67 g COD · (g COD·d)$^{-1}$	k_{m,Ge^-}	0.03 g COD · (g COD·d)$^{-1}$
$f_{l,g}$	0.68 g COD · (g COD)$^{-1}$	$k_{G,L}$	1.72 g COD · (g COD·d)$^{-1}$		
$f_{a,g}$	0.50 g COD · (g COD)$^{-1}$	K_{S_G}	1.9 g COD Glucose · l^{-1}		
$f_{H2a,g}$	0.50 g COD · (g COD)$^{-1}$	K_{S_E}	1.0 g COD Ethanol · l^{-1}		
$f_{b,g}$	0.83 g COD · (g COD)$^{-1}$	K_G	5.8 g COD Glucose · l^{-1}		

	Open circuit MFC	Ethanol MFC	Closed circuit MFC
Calibration data	15.1	21.5	10.5
Validation data			12.3

Figure 1. A concept of the bio-electro-chemical model based on the glucose fermentation, supplemented with the glucose and ethanol oxidation with electron-transfer to the electrode.

Figure 2. Schematic view of the H-type MFC set-up.

Figure 3. Performance of the H-type MFC under open circuit conditions (Solid lines correspond to model predictions).

Figure 4. Voltage generation and theoretical COD consumption rate in the H-type MFC fed with glucose (Solid lines correspond to voltage prediction).

Figure 5. Substrate and main products profiles during the closed circuit experiment (Solid lines correspond to model predictions).

Figure 6. Electricity generation and ethanol concentration profile in the MFC feed with ethanol (Solid lines correspond to model predictions).

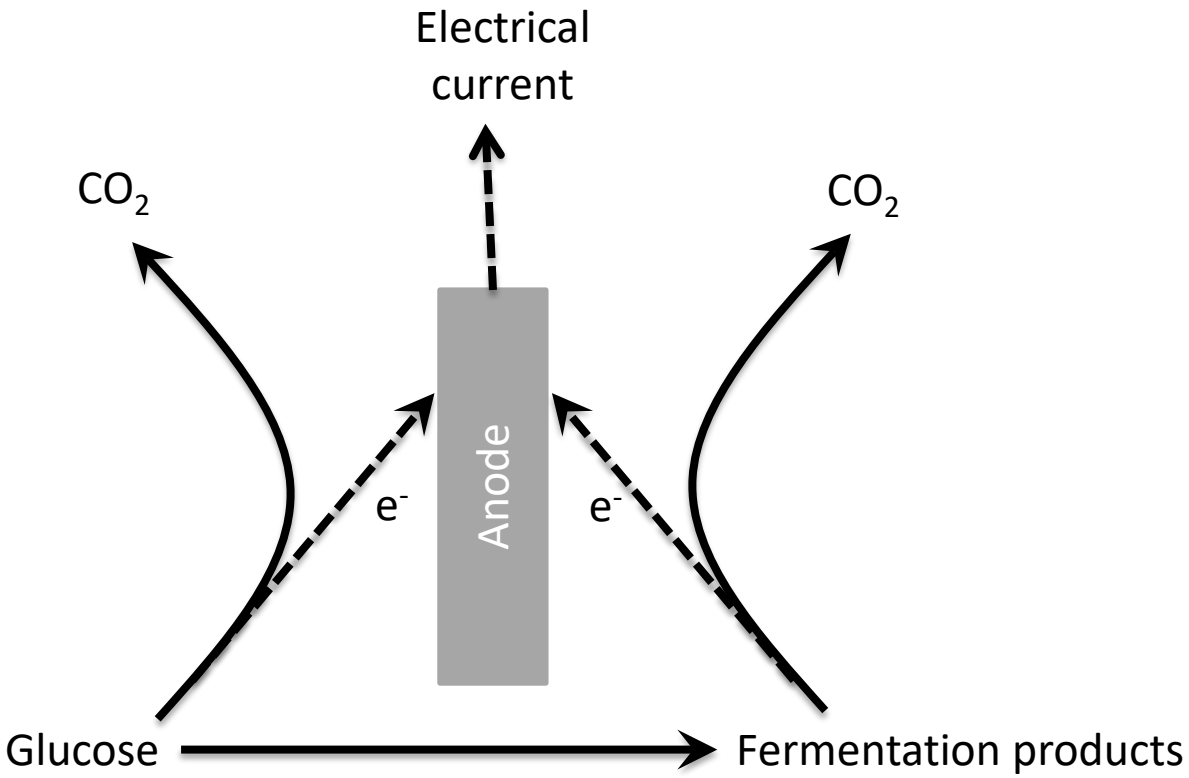

Figure 1. A concept of the bio-electro-chemical model based on the glucose fermentation, supplemented with the glucose and ethanol oxidation with electron-transfer to the electrode.

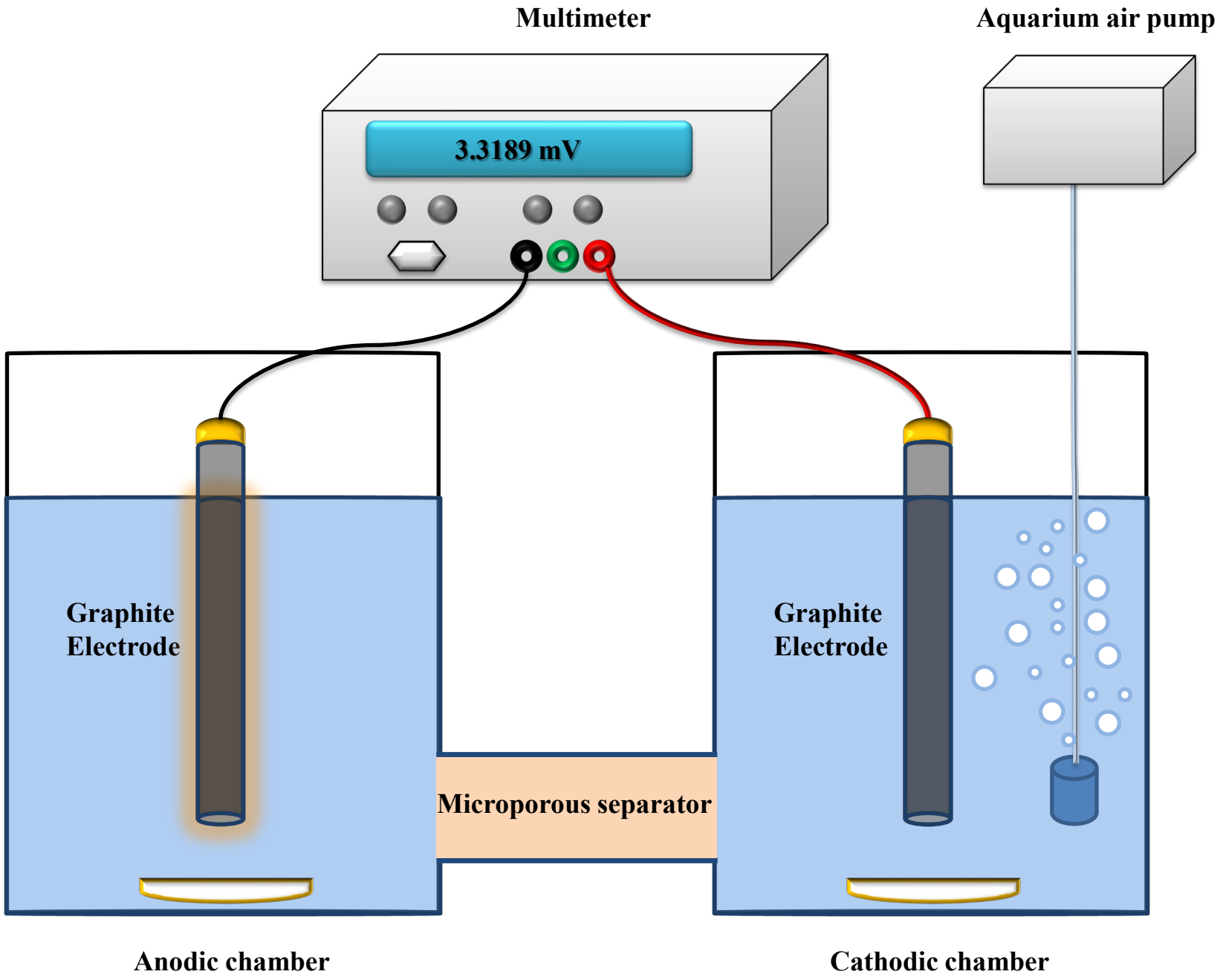

Figure 2. Schematic view of the H-type MFC set-up.

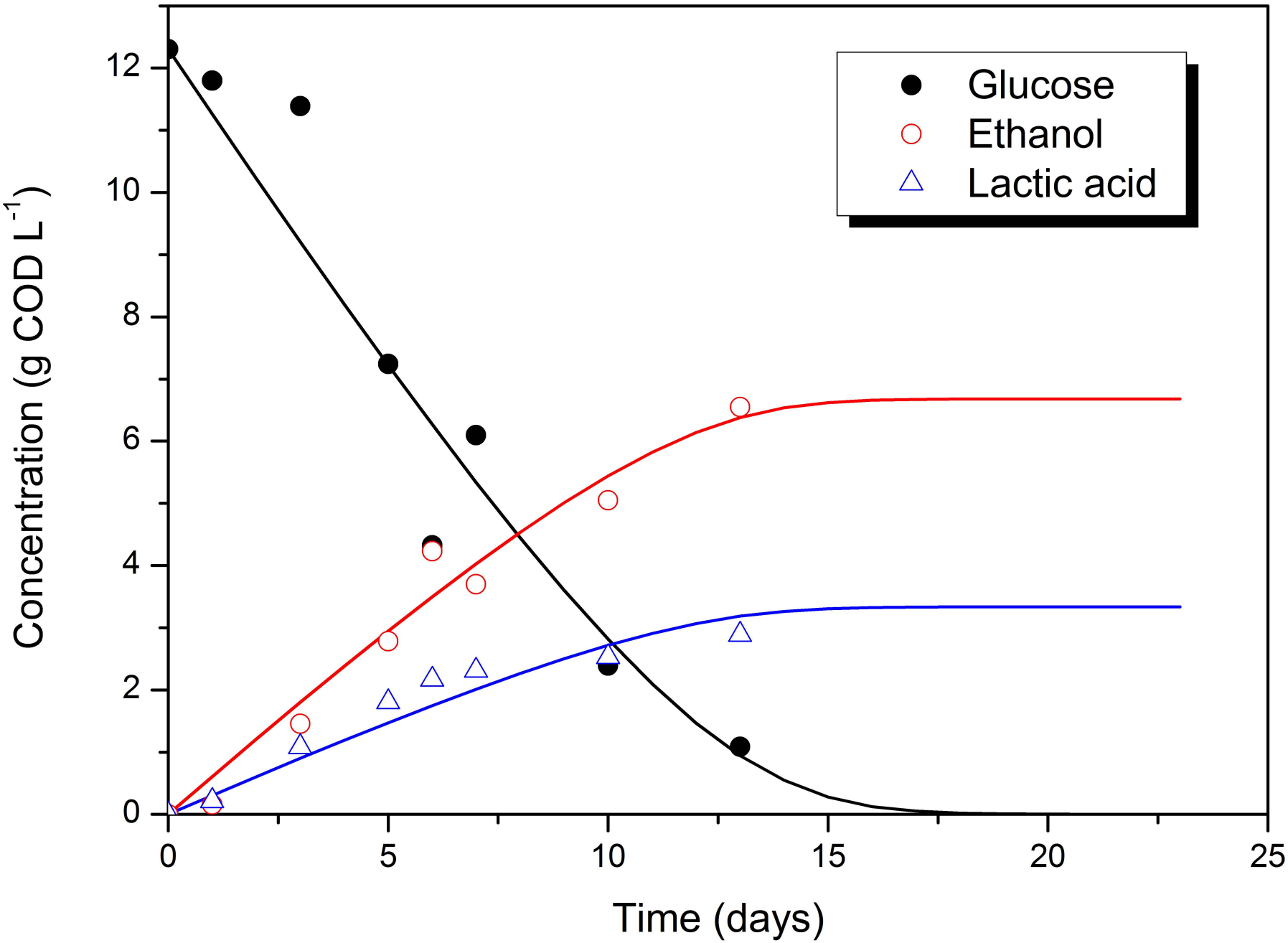

Figure 3. Performance of the H-type MFC under open circuit conditions (Solid lines correspond to model predictions).

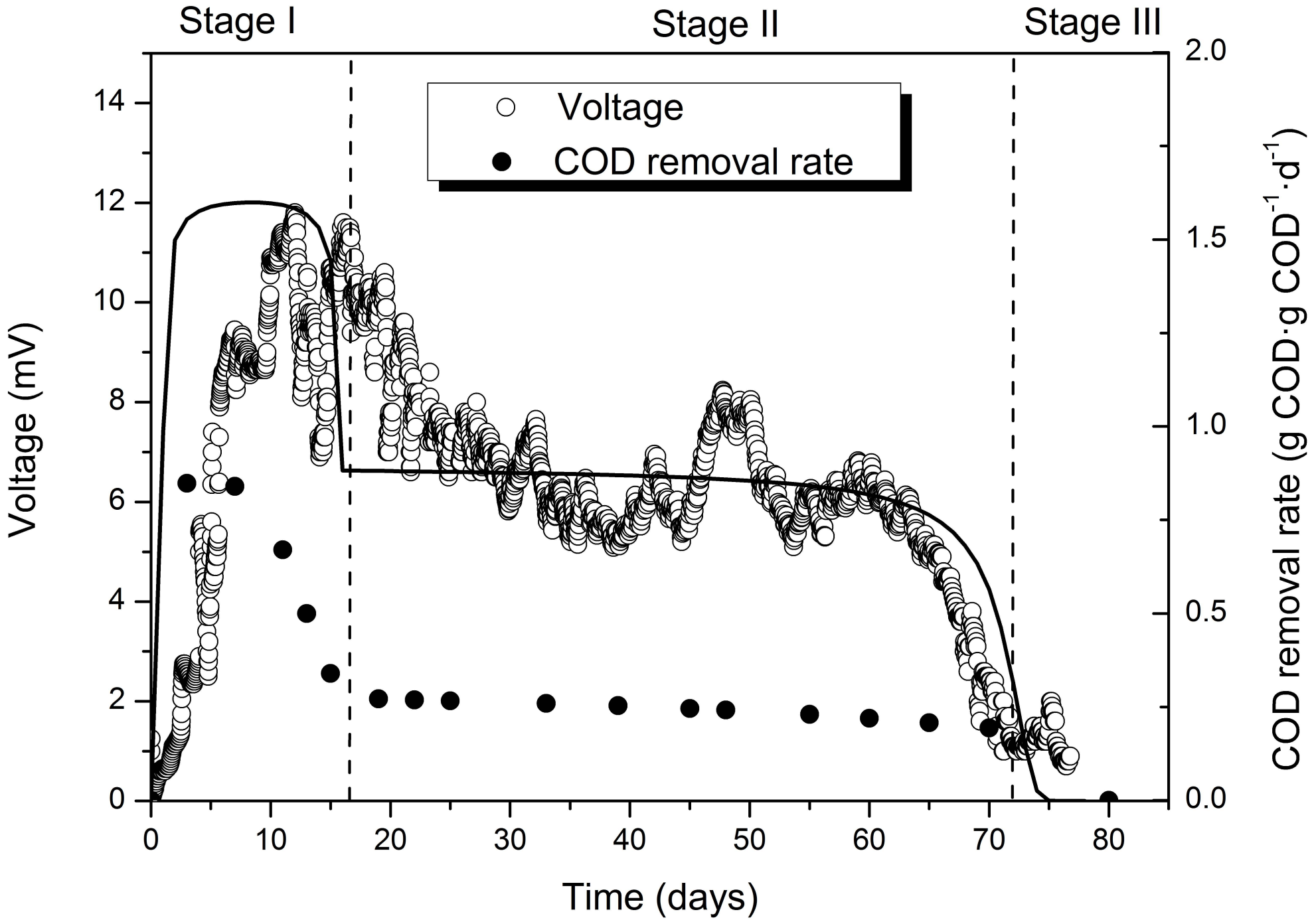

Figure 4. Voltage generation and theoretical COD consumption rate in the H-type MFC fed with glucose (Solid lines correspond to voltage prediction).

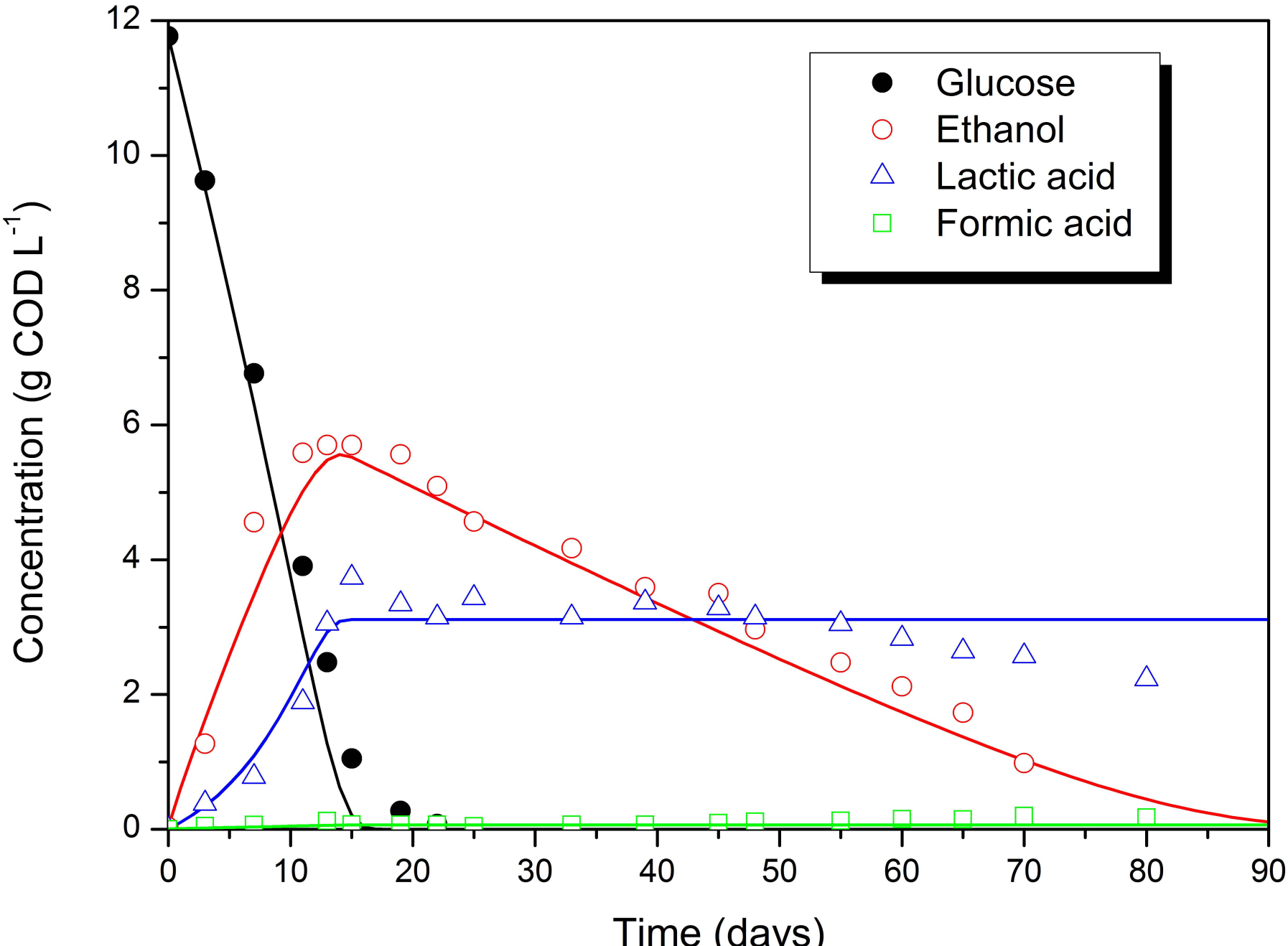

Figure 5. Substrate and main products profiles during the closed circuit experiment (Solid lines correspond to model predictions).